Study of Gas Phase m-Cresol Alkylation with Methanol on Solid Acid Catalysts

M. D. Acevedo, G. A. Bedogni, N. B. Okulik & C. L. Padró

Catalysis Letters

ISSN 1011-372X
Volume 144
Number 11

Catal Lett (2014) 144:1946-1954
DOI 10.1007/s10562-014-1358-6

Springer

Catal Lett (2014) 144:1946–1954
DOI 10.1007/s10562-014-1358-6

Study of Gas Phase m-Cresol Alkylation with Methanol on Solid Acid Catalysts

M. D. Acevedo · G. A. Bedogni · N. B. Okulik · C. L. Padró

Received: 7 July 2014 / Accepted: 26 August 2014 / Published online: 17 September 2014

Abstract The gas-phase alkylation of m-cresol with methanol was studied at 523 K on Al-MCM-41 and zeolites ZnY, HBEA, HZSM5 and HMCM22. The acidity was determined by ammonia TPD and FTIR of adsorbed pyridine. On acid sites of moderate strength (Al-MCM-41), initially the O-alkylation rate was higher than the C-alkylation rate. In contrast, formation of dimethylphenols by C-alkylation was highly favored on ZnY and HMCM22 which have both strong acidity although different nature; Lewis (ZnY) and Brønsted and Lewis (HMCM22). High selectivity of 2,5-DMP was observed on HZSM5, probably due to diffusional constraint. All catalysts, except Al-MCM-41, showed deactivation by coke formation.

Keywords Alkylation · Acid zeolites · m-Cresol methylation · Methylation · Solid acids catalysts · Dimethyl-phenols

1 Introduction

The alkylation of m-cresol with different alkylating agents can be considered a reaction of industrial relevance, mainly because of the valuable products obtainable therefrom. For example, the alkylation of m-cresol with 2-propanol, produces thymol, which has antiseptic properties, antimicrobial activity and is also intermediate in menthol synthesis [1]. Moreover, the alkylation of m-cresol with propanol, propanal and acetone was investigated as a useful reaction in the bio-oil production from biomass pyrolysis because it allows retaining carbon from small oxygenates fraction [2].

Using methanol, compounds like dimethyl-phenols (DMP) and 3 methyl-anisole (3-MA), can be produced by C-alkylation and O-alkylation, respectively (Scheme 1). Trimethylphenols (TMP) and dimethylanisoles (DMA) could be formed by successive alkylation. Among the dimethylphenols, 2,3-DMP is used in pesticides production, 3,4-DMP is raw material in the insecticide 3,4-dimethylphenyl methylcarbamate synthesis and 2,5 DMP is starting material in the manufacture of pharmaceuticals such as gemfibrozil (an oral drug used to lower lipid levels) and is also intermediate in synthesis of colorants, antiseptics and antioxidants [3]. Furthermore, one of the trimethylphenols, 2,3,6-TMP, is employed in α-tocopherol (vitamin E) synthesis, used as medicine and also as an antioxidant in stabilization of food, cosmetic and plastics.

The use of catalysts basic, redox and acids with moderate strength, such as MgO, Mg/Me (Al, Fe, Cr)-mixed oxides and V_2O_5, in m-cresol methylation, has been fairly studied in both liquid and gas phase [4–10]. In gas phase, the reaction was carried out typically at temperatures higher than 573 K, however, under these conditions, methanol decomposed becoming necessary to feed this reactant in a large excess over the stoichiometric relationship. Basic catalysts showed high chemo selectivity producing only minor amount of O-alkylation product and also regio-selectivity, being the *ortho*-isomer favored. Mg/Al-mixed oxide, which have no redox characteristics,

M. D. Acevedo · C. L. Padró (✉)
Catalysis Science and Engineering Research Group (GICIC), Instituto de Investigaciones en Catálisis y Petroquímica - INCAPE-(UNL-CONICET), Santiago del Estero 2654, (3000), Santa Fe, Argentina
e-mail: cpadro@fiq.unl.edu.ar
URL: http://www.fiq.unl.edu.ar/gicic

G. A. Bedogni · N. B. Okulik
Universidad Nacional del Chaco Austral, Comandante Fernández 755, CP 3700 Pcia. Roque Sáenz Peña, Chaco, Argentina

Scheme 1 Reaction network for methylation of m-cresol on solid acids

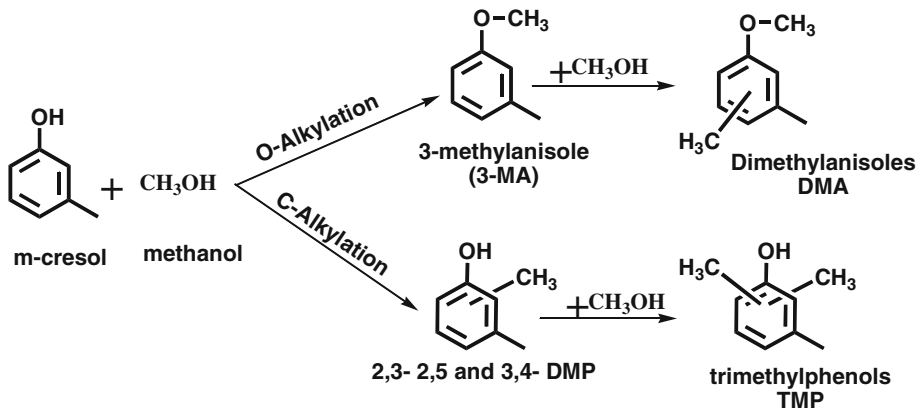

exhibited catalytic behavior similar to Brønsted-type acid catalysts: high selectivity to 3-methyl-anisole at low temperature (low conversion) that decrease as the temperature (conversion) increase becoming 2,5 DMP, 2,3 DMP and trimethylphenols main products of reaction [8].

Catalyst with redox characteristics like Mg/Cr/O, Mg/Fe/O or Fe/SiCr/O have shown high chemo- and regioselectivity: on these catalysts, 3-MA was not formed while high yields of 2,5 and 2,3-DMP were achieved at temperatures between 628 and 673 K [4, 8, 10].

Otherwise, it has been reported that solid acid catalysts such as SiO_2–Al_2O_3 are active at lower temperature if compared with catalysts based on MgO, but the absence of regio/chemo selectivity along with deactivation have been considered major drawbacks [5, 6, 8]. However, there is insufficient information about the methylation of m-cresol on solid acids, particularly, about the acid sites requirement to efficiently promote the C-alkylation. The alkylation of phenol with methanol instead, has been widely studied over acid catalysts and it was reported that on strong Brønsted acid sites O-alkylation is favored over the C-alkylation [11], while catalysts with the simultaneous presence of strong Brønsted and Lewis acid sites promote efficiently the formation of cresols [12].

In this paper we studied the alkylation of m-cresol with methanol on Al-MCM-41 and zeolites HMCM22, HBEA, HZSM5 and ZnY. The aim of our work was to ascertain the effect of the nature and strength of superficial acid sites on the catalytic activity and product distribution.

2 Experimental

2.1 Catalyst Preparation

Commercial samples of zeolites HZSM5 (Zeocat Pentasil PZ-2/54, Si/Al = 20) and HBEA (Zeocat PB/H) were used. Zeolite ZnY was obtained by triple ion exchange of zeolite NaY (UOP-Y 54, Si/Al = 2.4, 7.5 wt% of Na) with 0.5 M $Zn(NO_3)\cdot 6H_2O$ (Riedel-de Haën, 98 %) solution at 353 K. Zeolite HMCM22 was synthesized according to Ref. [13] by using sodium aluminate (Alfa Aesar, Technical Grade), silica (Aerosil Degussa 380), sodium hydroxide (Merck, >99 %), hexamethyleneimine (Aldrich, 99 %) and deionized water as reagents. The mesoporous solid Al-MCM-41 was prepared by sol–gel method, as reported by Edler and White [14].The reagents used in this work were: sodium silicate (Aldrich, 14 % NaOH, 27 % SiO_2) and aluminum isopropoxide (Aldrich, ≥98 %) as source of silicon and aluminum respectively, cetyltrimethylammonium bromide (CTABr, Sigma-Aldrich, ≥98 %) as surfactant and distilled water (molar gel composition: $7SiO_2$–$0.2Al_2O_3$–$2.7Na_2O$–$3.7CTABr$–$1000H_2O$). After crystallization, the solids (Al-MCM-41 and HMCM22 precursors) were filtered, washed with distilled water, dried in oven at 373 K and finally treated at 773 K in N_2 (6 h) and air (6 h). Before reaction, all the samples were treated in air (60 cm^3min^{-1}) at 723 K during 3 h.

2.2 Catalysts Characterization

BET surface areas were measured by physisorption of N_2 at 77 K in a Autosorb Quantochrome Instrument 1-C sorptometer. The chemical composition of the samples were determined by inductively coupled plasma atomic emission spectroscopy (ICP-AES) instrument, model 2000-DV (Perkin Elmer).

Density of surface acid sites was determined by temperature-programmed desorption (TPD) of NH_3. Samples were treated in helium at 773 K for 2 h, cooled down to 373 K then exposed to a 1 %NH_3–99 %He mixture. The physisorbed NH_3 was eliminated by flushing with He at 373 K during 90 min. Finally, the temperature was increased at 10 K min^{-1} in a He flow of 60 cm^3 min^{-1} and desorbed ammonia was analyzed by mass spectrometry (MS) in a Baltzers Omnistar unit.

Nature and strength of surface acid sites were studied by Infrared Spectroscopy (IR) using pyridine as probe molecule in a Shimadzu FTIR Prestige-21 spectrophotometer. The catalysts were ground to a fine powder and pressed into circular wafers of 13 mm of diameter (13–15 mg) in absence of binder. The discs were mounted in a quartz sample holder and transferred to an inverted T-shaped Pyrex cell equipped with CaF_2 windows. The samples were outgassed in vacuum at 723 K during 2 h and cooled to 298 K under evacuation. Spectra, average of 40 runs, were recorded at room temperature, after admission of pyridine, adsorption at room temperature and sequential evacuation at 423 and 573 K. The resolution used in all experiments was 4 cm^{-1}. The spectrum recorded after treatment and before pyridine adsorption, corresponding to the "clean" sample, was taking as a reference spectrum.

Coke formed on the catalysts during reaction was studied by temperature programmed oxidation (TPO). Catalysts recovered from reaction (20–100 mg) were heated from room temperature to 1,073 K at 10 K min^{-1} in a 2 %O_2–98 %N_2 stream. The evolved CO_2 was converted into methane passing through a methanation catalyst (Ni/kieselghur) at 673 K. Methane was analyzed using a flame ionization detector (gas chromatograph: SRI 310C).

2.3 Catalytic Activity

The gas phase alkylation of m-cresol (Sigma-Aldrich, >98 %) with methanol (Merck, 99.8 %) was carried out in a fixed bed continuous flow reactor at 523 K and 101.3 kPa. Catalysts (0.35–0.42 mm) were treated in situ at 723 K in air flow for 2 h before reaction. m-Cresol and methanol were fed as a solution (molar ratio Methanol/m-Cresol = 5) using a syringe pump (Cole-Parmer EW-74900) and vaporized in a preheated N_2 stream to give a N_2/(m-Cresol + Methanol) ratio of 37. The exit gas composition was analyzed on-line every 20 min during 4 h using an UNICAM 610 chromatograph equipped with a flame ionization detector and a 30 m Innowax column (inner diameter: 0.32 mm, film thickness: 0.5 μm). Main reaction products were dimethylphenols (2,5-, 2,3- and 3,4-DMP), 3-methylanisole (3-MA) and products formed by overalkylation: trimethylphenols (TMP) and dimethylanisoles (DMA). Moreover, compounds from dehydration and condensation of methanol, such as dimethylether (DME) and light hydrocarbons, were also observed.

m-Cresol conversion ($X_{m\text{-}Cresol}$) and Methanol conversion ($X_{Methanol}$) were calculated as: $X_{m-Cresol,Methanol} = (Y^0_{m-Cresol,Methanol} - Y_{m-Cresol,Methanol})/Y^0_{m-Cresol,Methanol}$ where $Y^0_{m-Cresol}$ and $Y^0_{Methanol}$ are the molar fraction of m-Cresol and Methanol at the entrance of the reactor while $Y_{m-Cresol}$ and $Y_{Methanol}$ are the molar fraction at the exit. The selectivity to product *i* formed from m-cresol molecules (S_i, mol of product *i*/mol of m-cresol reacted) was determined as: $S_i = [Y_i/\Sigma Y_i]$ where Y_i is the molar fraction of products formed from m-Cresol. Yields (η_i, mol of product *i*/mol of m-cresol fed) were obtained as $\eta_i = S_i \cdot X_{m-Cresol}$.

Table 1 Chemical composition and surface area of the samples used in this work

Samples	Chemical composition			
	Na (wt%)	Zn (wt%)	Si/Al	S_{BET} (m^2 g^{-1})
HBEA	0.04	–	12.5	560
HZSM5	0.43	–	20	350
ZnY	0.4	9.3	2.4	612
HMCM22	–	–	15.0	400
Al-MCM-41	–	–	18	205

3 Results and Discussion

3.1 Catalyst Characterization

The chemical composition and surface area of the catalysts are shown in Table 1. The exchange of zeolite NaY with Zn^{2+} cations diminished the sodium content from 7.5 to 0.4 wt%, which corresponds to exchange degree of 95 %. The exchange treatments decreased the surface area of parent NaY zeolite (700 m^2 g^{-1}) to 612 m^2 g^{-1} (ZnY). HMCM22 zeolite, prepared in our lab, was characterized by XRD before and after calcination. The peak positions and intensities of both diffractograms are in good agreement with those reported in the literature [13] proving that pure HMCM22 has been obtained.

The sample acidity was studied by NH_3 TPD and FTIR using pyridine as a probe molecule. The acid sites densities (μmol g^{-1}) were determined by deconvolution and integration of the NH_3 TPD profiles (not shown here) and are included in Table 2. The densities of surface acid sites determined on HZSM5, HMCM22 and HBEA were similar (between 470–500 μmol g^{-1}). Zeolites ZnY showed the highest concentration of acid sites per gram (1,787 μmol g^{-1}) whereas Al-MCM-41 presented the lowest acidity (135 μmol g^{-1}).

The nature and strength of surface acid sites were studied by FTIR after adsorption of pyridine at 298 K and evacuation at 423 K and 573 K. Pyridine adsorbed on Brønsted acid sites shows absorption bands at 1,540 cm^{-1}, 1,480–1,500 cm^{-1} and 1,640 cm^{-1}, whereas pyridine coordinatively bonded on Lewis acid sites produces characteristic bands at 1,440–1,460 cm^{-1}, 1,480–1,500 cm^{-1} and 1,600 cm^{-1}[15–17]. The difference between FTIR spectra after evacuation of pyridine at 423 K and reference spectra

Table 2 Sample Acidity

Sample	TPD of NH_3	FTIR of pyridine					
	Acid site density (μmol g^{-1})	$T_{desorption} = 423$ K			$T_{desorption} = 573$ K		
		Brønsted concentration (C_B) (μmol g^{-1})	Lewis concentration (C_L) (μmol g^{-1})	C_L/C_B	Brønsted concentration (C_B) (μmol g^{-1})	Lewis concentration (C_L) (μmol g^{-1})	C_L/C_B
HBEA	500	307	185	0.6	295	73	0.2
HZSM5	475	268	205	0.8	228	93	0.4
ZnY	1,787	29	720	24.5	7	528	73.9
HMCM22	470	445	106	0.2	353	72	0.2
Al-MCM-41	135	12	33	2.8	2	32	20.0

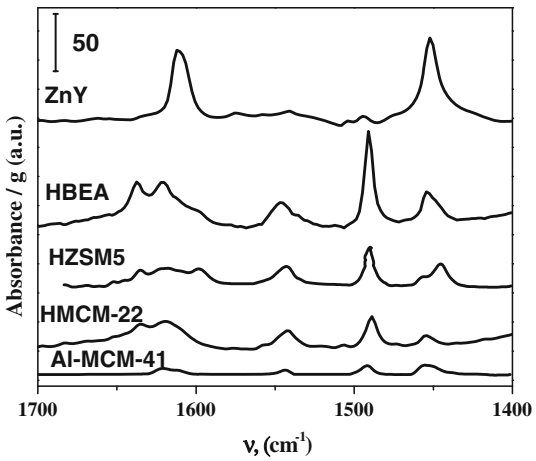

Fig. 1 IR difference spectra of adsorbed pyridine at 298 K and evacuated at 423 K for 0.5 h

("clean" sample) are displayed in Fig. 1. Zeolite ZnY presented essentially Lewis acidity, main bands in spectrum are absorption bands at 1,455 and 1,615 cm^{-1} corresponding to pyridine coordinatively bound on Zn^{2+} cations [18, 19]. Spectrum in Fig. 1 shows on Al-MCM-41 the bands at 1,617 cm^{-1} and 1,455 cm^{-1}, which reflects the adsorption of pyridine on Lewis acid sites associated with tricoordinate Al atoms [20]. It was also observed some Brønsted acidity: small bands at 1,540 and 1,625 cm^{-1}. FTIR spectra of zeolites HZSM5, HBEA and HMCM22 revealed the presence of both Lewis (bands at 1,455 and 1,620 cm^{-1}) and Brønsted acid sites (bands at 1,540 and 1,635 cm^{-1}).

The concentrations of Brønsted and Lewis acid sites (C_B and C_L, μmol g^{-1}) after evacuation of pyridine at 423 and 573 K were estimated from the area of the IR characteristic bands 1,540–1,550 cm^{-1} (A_B) and 1,440–1,450 cm^{-1} (A_L) using the equations derived by Emeis [21]:

$$C_B = 1.88 \frac{A_B \cdot R^2}{W} \quad (1)$$

$$C_L = 1.42 \frac{A_L \cdot R^2}{W} \quad (2)$$

where R (cm) is the radius of catalyst disk and w (g) is the weight of the dry sample. Results are presented in Table 2.

The integrated molar extinction coefficients calculated in Ref. [21] apply to Si/Al-based catalysts and a measurement temperature of 423 K. However, it has been indicated that these coefficient do not depend markedly on recording temperature and they are slightly modified with the adsorption temperature [22–24], making acceptable their application to our results.

Al-MCM-41 retained small amount of pyridine even after evacuation at 423 K revealing the weak nature of the acid sites. After outgassing at 423 K, C_L/C_B ratios of 0.6, 0.8 and 0.2 were determined for zeolites HBEA HZSM5 and HMCM22, respectively. The Py-523 K/Py-423 K ratios (i.e. the ratio of the amounts of pyridine remaining on the samples after evacuation at 523 and 423 K) were 0.77, 0.65 and 0.7 on HMCM22, HZSM5 and HBEA, respectively, thereby indicating that HMCM22 presented stronger acid sites mainly of Brønsted nature. Zeolite ZnY contains mostly Lewis acid sites ($C_L/C_B = 24.5$ and 73.9 after desorption at 423 K and 523 K, respectively) that retain significant amount of pyridine after evacuation at 523 K. In fact the Py-523 K/Py-423 K ratio calculated for this catalyst was 0.72 denoting the significant strength of these acid sites.

3.2 Catalytic Results for Methylation of m-Cresol

3.2.1 Catalyst Activity and Deactivation

Catalysts were tested in gas phase methylation of m-cresol at 523 K. In Fig. 2, we plotted the m-cresol and methanol conversions (X_i) and products selectivities (S_i) as a function of time obtained on ZnY using a contact time of $W/F^0_{m-Cresol}$

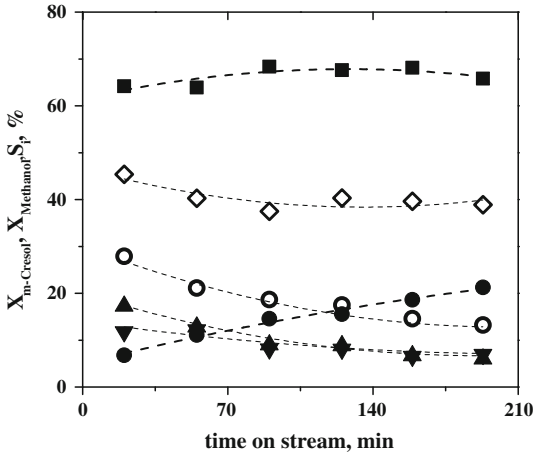

Fig. 2 m-Cresol and Methanol conversions ($X_{m\text{-}Cresol}$, $X_{Methanol}$) and Selectivities (S_i) as a function of time-on-stream on ZnY [523 K, $P_T = 101.3$ kPa, $W/F^0_{m-Cresol} = 181$ g h mol^{-1}, $P_{m\text{-}cresol} = 0.44$ kPa, $P_{methanol} = 2.23$ kPa] 0 P F/W $X_{m\text{-}Cresol}$ (*open circle*), $X_{Methanol}$ (*open diamond*), S_{3MA} (*filled circle*), S_{DMP} (*filled square*), S_{DMA} (*filled nabla*), S_{TMP} (*filled triangle*)

= 181 g h mol^{-1}, as an example of typical time-on-stream behavior of the catalysts studied in this work. m-Cresol conversion ($X_{m\text{-}Cresol}$) decreased with time evidencing the in situ deactivation of ZnY. A diminution in methanol conversion was observed as well, even though it was considerably lower. Initial selectivity to dimethylphenols, was 62 % and increased to $S_{DMP} = 67$ % at 3 h of reaction. The $S_{3\text{-}MA}$ also increased with time from 5.1 to 21 %, whereas selectivities to trimethylated products (S_{TMP} and S_{DMA}) instead, decreased consistent with a secondary products typical behavior.

Due to catalyst deactivation observed in Fig. 2, initial catalytic results on fresh catalysts were obtained by extrapolating the corresponding curves to $t = 0$. m-Cresol conversions at zero time and after 3 h of reaction obtained at 523 K and same contact time ($W/F^0_{m-Cresol} =$ 181 g h mol^{-1}) are displayed in Table 3. Initially, HBEA was more active than the rest of the catalysts employed in this work, reaching 95 % of m-cresol conversion at the beginning of reaction. Despite containing similar density of superficial acid sites than HBEA, HMCM22 and HZSM5 zeolites were significantly less active. In fact, we have calculated the TOF values (ratio between initial m-cresol conversion rate and acid site density), which are 10 h^{-1}, 1.2 h^{-1} and 1.7 h^{-1} for HBEA, HZSM5 and HMCM22 respectively. The low values found for HZSM5 and HMCM22 are probably due to diffusional constraint inside of the narrow pores of both zeolites. These results are expectable if it is considered that previous works have proved the intracrystalline diffusion control in phenol methylation for both catalysts [12, 25, 26]. ZnY and Al-MCM-41, that contain almost exclusively Lewis acid sites, were active in the reaction, although the conversions were considerably lower than on HBEA ($X^0_{m-Cresol} = 33$ and 10 %, respectively), revealing that Lewis acid sites, even of moderate-weak strength as in Al-MCM-41, are suitable to promote the methylation of m-cresol. Actually, the TOF value calculated for Al-MCM-41 (4 h^{-1}), catalyst that does not have diffusion limitation, was four times the value obtained for ZnY (1.0 h^{-1}).

By observing the m-cresol conversion after 3 h of reaction, it can be inferred that all samples, except Al-MCM-41, deactivated on stream. It is worth noting that on Al-MCM-41, no noticeable activity decay was observed during the reaction, exhibiting a different behavior than the rest of the catalysts tested in this work.

Catalyst deactivation could be caused by coke formation from parallel/consecutive reaction of reactants or products. The carbon deposited on the catalyst recovered after the catalytic tests at same contact time, was studied by TPO and the C % is presented in Table 3. ZnY and HBEA formed the highest amount of carbon (12.2 and 11.5 %, respectively) while the lowest amount of coke (2.1 %) was formed on Al-MCM-41, which did not deactivate on stream, thereby indicating that the coke is responsible for the loss of activity observed. In previous works, it has been suggested that deactivation on acid solids is caused by parallel reactions that involved the alkylating agent. Methanol can be transformed both on acid or basic/redox catalysts [8]. While on basic/redox catalyst, methanol is dehydrogenated to formaldehyde and subsequent formation of CO or CH_4 and CO_2, on acid catalysts, it undergoes dehydration and condensation to DME (on either Brønsted or Lewis sites) and by successive self-oligomerization, light hydrocarbons and aromatics are formed, which are coke precursors. In fact, formation of carbon deposits from methanol on solid acids has been previously studied [27–29].

All the catalysts used in this work are able to activate methanol as inferred from the values of methanol conversion in Table 3. Indeed, methanol conversions varied form 46 % on ZnY to 81 % on HBEA at time zero. Taking into account the methanol to m-cresol molar ratio used in the feed (Methanol/m-Cresol = 5), from this results it is possible to deduce that high amount of methanol was converted in parallel reactions to form DME and light hydrocarbons. In fact, in all our catalytic runs we have detected DME and hydrocarbons.

Additional experiments were performed in order to establish whether the methanol or m-cresol could form coke by itself on ZnY or the simultaneous presence of both reactants is required. Methanol and/or m-cresol were feeding in a N_2 stream. The coke formed on the recovered samples after 3 h, as well as the coke formed during the methanol/m-cresol reaction in similar conditions, were determined by TPO. We have selected ZnY for these

Table 3 Catalytic results for the alkylation of m-cresol with methanol

Catalyst	m-Cresol conversion, $X_{m\text{-}Cresol}$ (%)[a]		Methanol conversion, $X_{Methanol}$ (%)[a]		C[c] (%)	Selectivity ($X_{m\text{-}cresol}$ = 20 %, t = 0) (%)[b]				DMP isomer distribution ($X_{m\text{-}cresol}$ = 20 %, t = 0) (%)		
	t = 0 h	t = 3 h	t = 0 h	t = 3 h		3-MA	DMP	TMP	DMA	2,5 DMP	2,3 DMP	3,4 DMP
HBEA	95.0	33.0	81	47	11.5	28	51	14	7	38	32	30
HZSM5	10.0	1.0	56	51	7.8	22	71	5	2	71	15	14
ZnY	33.0	13.0	46	39	12.2	7	76	13	4	49	22	29
HMCM22	15.0	2.0	63	31	8.0	7	90	3	0	44	33	23
Al-MCM-41	10.0	8.0	50	40	2.1	56	37	5	2	33	37	30

[a] 523 K, P_T = 101.3 kPa, $P_{m\text{-}cresol}$ = 0.44 kPa, $P_{methanol}$ = 2.23 kPa, $W/F^0_{m-Cresol}$ = 181g h mol^{-1}

[b] 523 K, P_T = 101.3 kPa, $P_{m\text{-}cresol}$ = 0.44 kPa, $P_{methanol}$ = 2.23 kPa

[c] Carbon formed after 3 h of reaction as determined by TPO

Table 4 Coked formed after 3 h of reaction on ZnY

Reactants	% C
Methanol[a]	2.4
m-Cresol[b]	2.2
m-Cresol + methanol[c]	15

[a] 523 K, P_T = 101.3 kPa, $P_{methanol}$ = 2.23 kPa, $W/F^0_{methanol}$ = 18.1g h mol^{-1}

[b] 523 K, P_T = 101.3 kPa, $P_{m\text{-}cresol}$ = 0.44 kPa, $W/F^0_{m-Cresol}$ = 90.5g h mol^{-1}

[c] 523 K, P_T = 101.3 kPa, $P_{m\text{-}cresol}$ = 0.44 kPa, $P_{methanol}$ = 2.23 kPa, $W/F^0_{m-Cresol}$ = 90.5gh mol^{-1}

experiments considering two facts: (i) ZnY formed the greatest amount of coke during the reaction (Table 3) (ii) even though the reactions of m-cresol (isomerization and disproportionation) and methanol to hydrocarbons have been widely studied over acid catalysts with essentially Brønsted nature [28–32], there is lack of information about these reactions on Lewis acid catalysts. It can be observed in Table 4 that the amount of carbon deposits on the samples that were fed with methanol or m-cresol alone (2.4 or 2.2 % of C) was considerably lower than coke formed under the simultaneous presence of methanol and m-cresol (15 % of C). Therefore, the carbon deposit formation on this catalyst was not only originated from methanol but it involved reactions that require the presence of both reactants and likely also alkylated products. In this respect, it is noteworthy that retention of polyalkylated phenols has been proposed as one of the mechanism responsible for the progressive deactivation of similar catalysts in the methylation of phenol [19].

3.3 Catalyst Selectivity

In order to ascertain the relationship between the nature and strength of the acid sites and the products formed by alkylation, we desired to compare the products selectivities on fresh catalysts at a same m-cresol conversion level. To obtain these values, additional experiences were carried out at different contact times keeping unmodified the rest of the reaction conditions. Results at $X^0_{m-Cresol}$ = 20 % are included in Table 3. Main products formed were 3-MA and dimetylphenols (2,5- 2,3- and 3,4-DMP). Moreover, it was observed the formation of trimethylphenols (TMP, products of the C-methylation of DMP) and DMA (from C-alkylation of 3-MA or O-alkylation of DMP) in minor proportion. The scarce formation of trimethylated products (TMP and DMA) exhibited by HMCM22 and HZSM5 may be due to their narrow pore structures that prevent the formation of the bulky intermediates involved [26].

The C/O-alkylation ratio, i.e. the ratio between products from the alkylation in the aromatic ring (DMP and TMP) and the O-alkylation products (3-MA and DMA) was calculated for all the catalysts at same level of conversion ($X^0_{m-cresol}$ = 20 %) and is plotted in Fig. 3. On Al-MCM-41 (mostly acid Lewis sites of moderate strength) the main product of reaction was 3-MA ($S_{3\text{-}MA}$ = 56 %) giving a C/O-alkylation ratio of 0.72 which is the lowest value, followed by HBEA and HZSM5 (Fig. 3). In contrast, ZnY, which also contains almost exclusively Lewis sites but stronger than Al-MCM-41, formed mainly products alkylated in the aromatic ring (DMP, S_{DMP} = 76 % and TMP, S_{TMP} = 13 %) yielding a C/O alkylation ratio of 8.1. Selective C-alkylation of m-cresol on Lewis acid sites presents in $ZnAl_2O_4$ have been reported previously using isopropanol to produce thymol (2-isopropyl-5-methylphenol) [1]. The highest selectivity to products from C-alkylation was obtained on HMCM22 (C/O ratio of 13.3), thereby indicating that, solids with the presence of high strength acid sites (either Lewis or Brønsted nature) are capable to promote preferentially the alkylation in the aromatic ring.

Finally, Table 3 also shows the DMP isomer distribution. The occurrence of 3,5-DMP by substitution in *metha*

position, was not observed. On Al-MCM-41 and HBEA no preferential formation was observed, the substitution in *ortho* position (2,3 and 2,5 DMP) is twice than in *para*-(3,4-DMP), which corresponds to the statistical value. The DMP isomers distribution on ZnY showed a *ortho*-/*para*-ratio of 2.5, slightly higher than the statistical value, additionally, it can be observed that among the *ortho* substituted DMP, 2,5-was preferentially formed ($S_{2,5DMP}$/$S_{2,3DMP}$ = 2.2). Similar results were obtained on HMCM22. A noteworthy result is noticed on HZSM5: 71 % of DMP formed on this catalyst was 2,5-DMP, yielding a *ortho*-/*para*-ratio of 6.2 and $S_{2,5DMP}$/$S_{2,3DMP}$ = 4.6. This special behavior is probably explained by shape selectivity. The particular structure of HZSM5 zeolite, that has a three-dimensional channel system with elliptical aperture (5.1 × 5.5 Å) interconnected by zigzag channels with approximately circular cross section of 5.3 × 5.6 Å with no cages, in certain cases causes shape selectivity, i.e. the product distribution can be changed according to the ease of diffusivity of products. Comparing the relative dimensions of the isomers: 2,5-DMP, 2,3-DMP and 3,4-DMP (Fig. 4), we might speculate that 2,5 DMP would diffuse at higher rate than the other isomers inside the narrow channels of this zeolite. However, it has to be noted that it was not observed the same effect on HMCM22. Opposed results have been informed for phenol methylation [26]. *p*-Cresol (smallest cresol isomer) was

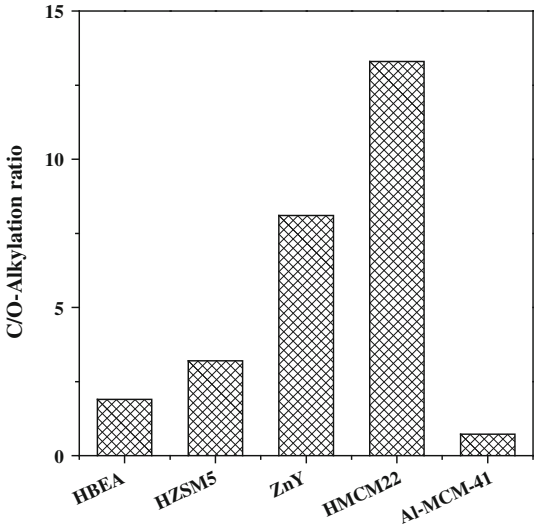

Fig. 3 C/O alkylation selectivity ratio compared at same level of m-cresol conversion [523 K, P_T = 101.3 kPa, $P_{m\text{-}cresol}$ = 0.44 kPa, $P_{methanol}$ = 2.23 kPa,]

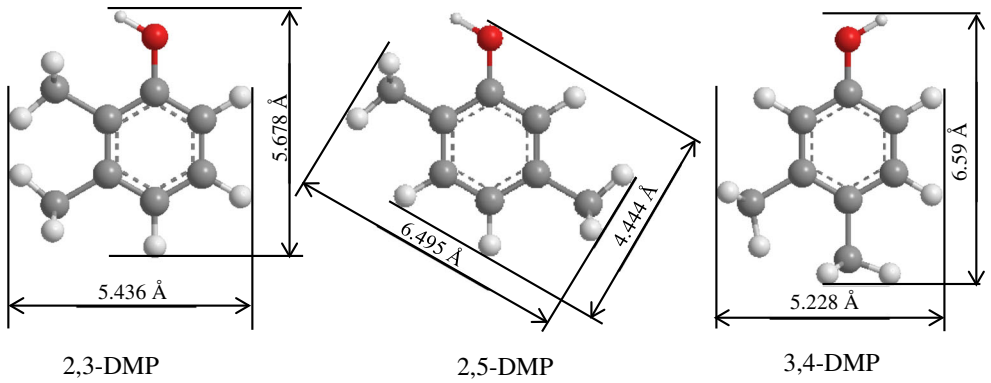

Fig. 4 Schematic representation of 2,3-DMP, 2,5-DMP and 3,4-DMP

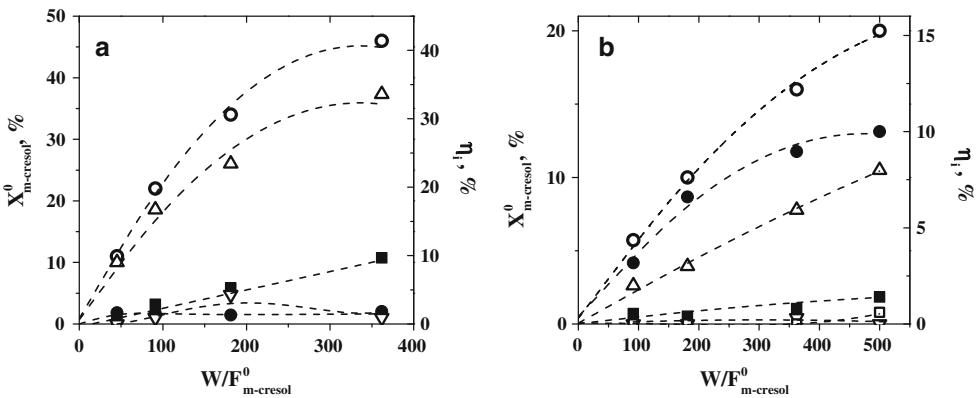

Fig. 5 Yields (η_i^0) and m-Cresol conversion ($X^0_{m-cresol}$) at $t = 0$ as a function of contact time for **a** ZnY, **b** Al-MCM-41 [523 K, PT = 101.3 kPa, Pm-cresol = 0.44 kPa, Pmethanol = 2.23 kPa] $X^0_{m-cresol}$ (*open circle*), η^0_{3-MA} (*filled circle*), η^0_{DMP} (*open triangle*), η^0_{DMA} (*open nabla*), η^0_{TMP} (*filled square*), η^0_{TMA} (*filled circle*)

selectively synthetized on HMCM22 while on HZSM5, the selectivity to *p*-cresol was not improved, even though DMP formation was hampered on both catalysts by diffusional constraints.

Additionally, we have investigated the effect of contact time on the product distribution on ZnY and Al-MCM-41. Yields (η_i^0) and m-cresol conversion ($X^0_{m-Cresol}$) at $t = 0$ are shown as a function of contact time in Fig. 5. Because of catalyst deactivation observed during the reaction, to obtain each data point on fresh catalyst, initial yields were determined by extrapolating to initial time on stream. The local slopes of the yield curves in Fig. 5 give the rate of formation of each product at a specific reactant conversion and contact time. The nonzero initial slopes of DMP and 3-MA yields evidence that these are primary products, formed directly by the attack of alkylating agent to m-cresol while the initial zero slopes observed for TMP, and DMA suggest that these compounds are secondary products formed by the alkylation of DMP and 3-MA. In fact, on ZnY, η^0_{3-MA} curve reaches a maximum, indicating that 3-MA, which is formed as primary product, then is converted to a secondary product.

In order to get more insight about the effect of the strength of the superficial acid sites, on promoting the different pathways involved in the reaction network (Scheme 1), we have calculated the initial rate of formation ($X^0_{m-cresol} \rightarrow 0$) of 3-MA (O-alkylation) and DMP (C-alkylation) from the slopes at $W/F^0_{m-cresol} \rightarrow 0$ in Fig. 5a and b. The values of r^0_{3-MA} calculated were 0.42 and 0.37 mmol h^{-1} g^{-1} while the values of r^0_{DMP} were 0.18 and 1.9 mmol h^{-1} g^{-1} on Al-MCM-41 and ZnY, respectively. Even though the initial rates of alkylation on the oxygen to form 3-MA were similar on both catalysts, the initial rate of C-alkylation was 10 times greater on the stronger sites of ZnY, proving that the C-alkylation require sites of high strength to proceed efficiently. Similarly, in previous papers, using Mg/Al mixed oxides, MgO or $SiO_2Al_2O_3$ as catalysts, it was found that C-alkylation is preferred over O-alkylation as the strength of the sites (either basic or acid catalytic sites) or the reaction temperature increases [5–7]. The reaction temperature in these works was between 573 and 823 K.

4 Conclusions

The solid acid catalysts studied in this paper were active for the gas-phase alkylation of m-cresol with methanol at 523 K. The catalytic activity and selectivity strongly depend on the nature and strength of the surface acid sites. HBEA, which contains acid sites of Brønsted and Lewis nature of considerable strength, is highly active but unselective forming 3-MA (C/O ratio of 1.9) and DMP in a statistics ratio, as well as trimethylated phenols: TMP and DMA. However, the selectivity can be tuned by modifying the nature and principally the strength of the acid sites. In fact, ZnY (strong Lewis acidity) promote selectively the C-methylation (C/O alkylation ratio: 8.8) leading to formation of 2,5, 2,3 and 3,4 DMP. In contrast, Al-MCM-41 (weak Lewis acidity) favors the O-alkylation reaching a selectivity value to the ether (3-MA) higher than 57 %. Highest selectivity to C-alkylated products (C/O alkylation ratio: 13.3) was obtained on HMCM22. This catalyst has strong acid sites mostly Brønsted (B/L = 3). On another hand, also by shape selectivity the product distribution can be modified. As a matter of fact, on HMCM22 and HZSM5 the production of TMP and DMA was hampered by diffusional constraint. Additionally on HZSM5, selectivity greater than 50 % to the smallest isomer of DMP, 2,5 DMP, could be explained by shape selectivity.

All the catalysts employed in this work form coke (between 2 and 12 %) and undergo significant losses of activity on stream, except Al-MCM-41. Although methanol participates in parallel reactions that lead to formation of light hydrocarbon and aromatics, it was proved that the simultaneous presence of both reactants is required for coke formation.

Acknowledgments This work was supported by the Universidad Nacional del Litoral (UNL), Consejo Nacional de Investigaciones Científicas y Técnicas (CONICET), and Agencia Nacional de Promoción Científica y Tecnológica (ANPCyT), Argentina.

References

1. Grabowska H, Mista W, Trawsczynski J, Wrzyszcz J, Zawadzki M (2001) Appl Catal A 220:207
2. Nie L, Resasco DE (2012) Appl Catal A 447:14
3. Fiege H (2012) Cresol and xylenols, Ullmann's encyclopedia of industrial chemistry. Wiley-VCH, Weinheim
4. Grabowska H, Wrzyszcz J, Syper L (1999) Catal Lett 57:135
5. Durgakumari V, Narayana S (1991) J Mol Catal 65:285
6. Durgakumari V, Sreekanth G, Narayanan S (1990) Res Chem Intermed 14:223
7. Bolognini M, Cavani F, Scagliarini D, Flego C, Perego C, Saba M (2002) Catal Today 75:103
8. Crocella V, Cerrato G, Magnacca G, Morterra C, Cavani F, Cocchi S, Passeri S, Scagliarini D, Flego C, Perego C (2010) J Catal 270:125
9. Cavani F, Maselli L, Scagliarini D, Flego C, Perego C (2005) In: Gamba A, Colella C, Coluccia S (eds) Studies in surface science and catalysis, vol 155, p 167
10. Crocellà V, Cerrato G, Magnacca G, Morterra C, Cavani FL, Maselli L, Passeri S (2010) Dalton Trans 39:8527
11. Santacesaria E, Grasso D, Gelosa D, Carra S (1990) Appl Catal 64:83
12. Sad ME, Padró CL, Apesteguía CR (2008) Catal Today 133–135:720
13. Rubin MK, Chu P (1990) US Patent 4.954.325
14. Edler KJ, White JW (1997) Chem Mater 9:1226

15. Parry EP (1963) J Catal 2:371
16. Knözinger H (1976) Adv Catal 25:184
17. Busca G (1998) Catal Today 41:191
18. Penzien J, Abraham A, van Bokhoven J, Jentys A, Müller T, Sievers C, Lercher JJ (2004) J Phys Chem B 108:4116
19. Padró CL, Rey EA, González Peña LF, Apesteguía CR (2011) Micropor Mesopor Mater 143:236
20. Sakthivel A, Dapurkar SE, Gupta NM, Kulshreshtha SK, Selvam P (2003) Micropor Mesopor Mater 65:177
21. Emeis CA (1993) J Catal 141:347
22. Barzetti T, Selli E, Moscotti D, Forni L (1996) J Chem Soc Faraday Trans 92:1401
23. Makarova MA, Karim K, Dwyer J (1995) Microporous Mater 4:243
24. Khabtou S, Chevreau T, Lavalley JC (1994) Microporous Mater 3:133
25. Santacesaria E, Di Serio M, Clambelli P, Gelosa D, Carra S (1990) Appl Catal 64:101
26. Sad ME, Padró CL, Apesteguía CR (2008) Appl Catal A 342:40
27. Knözinger H, Kochloeft K, Meye W (1973) J Catal 28:69
28. Knözinger H, Dautzenberg D (1974) J Catal 33:142
29. Tsoncheva T, Dimitrova R (2002) Appl Catal A 225:101
30. Imbert FE, Gnep N, Guisnet M (1997) J Catal 172:307
31. Chang C (1984) Cat Rev Sci Eng 26:323
32. Ilias S, Bhan A (2013) ACS Catal 3:18